Release of Sulfur and Chlorine during Cofiring RDF and Coal in an Internally Circulating Fluidized Bed

Xiaolin Wei,*,† Yang Wang,† Dianfu Liu,† Hongzhi Sheng,† Wendong Tian,‡ and Yunhan Xiao‡

Institute of Mechanics, and Institute of Engineering Thermophysics, Chinese Academy of Sciences, Beijing 100190, China

Received June 18, 2008. Revised Manuscript Received October 17, 2008

An internally circulating fluidized bed (ICFB) was applied to investigate the behavior of chlorine and sulfur during cofiring RDF and coal. The pollutant emissions in the flue gas were measured by Fourier transform infrared (FTIR) spectrometry (Gasmet DX-3000). In the tests, the concentrations of the species CO, CO_2, HCl, and SO_2 were measured online. Results indicated when cofiring RDF and char, due to the higher content of chlorine in RDF, the formation of HCl significantly increases. The concentration of SO_2 is relatively low because alkaline metal in the fuel ash can absorb SO_2. The concentration of CO emission during firing pure RDF is relatively higher and fluctuates sharply. With the CaO addition, the sulfur absorption by calcium quickly increases, and the desulfuration ratio is bigger than the dechlorination ratio. The chemical equilibrium method is applied to predict the behavior of chlorine. Results show that gaseous HCl emission increases with increasing RDF fraction, and gaseous KCl and NaCl formation might occur.

Introduction

Municipal solid waste (MSW) comprises combustibles (e.g., plastic, paper, textile, etc.), biomass with high moisture content (e.g., kitchen waste and wood, etc.), and noncombustibles (e.g., brick, ash, metal, etc.). According to the economical analysis, a hopeful treatment method of gaining maximum income is MSW integrating disposal technology, by which the three sorts of waste are disposed separately, that is, combustibles used to incinerate, biomass to compost, and noncombustibles to landfill or recycle. In this process of MSW disposal, combustibles are made as refuse-derived fuels (RDF), kitchen waste as fertilizer, and metal as recycling matter. This may bring considerable profits for an integrating disposal plant. Therefore, now such MSW disposal plants are being built in China. The production of RDF is growing as a potential fuel, and the pollution from RDF combustion should be a concern.

RDF has the advantage of high heating value and is easy to burn. One of the potential applications of RDF is cofiring with coal instead of some coal in the boiler. The faction of RDF in fuels has shared a 5−40% heating value in some boilers.[1−3] Because of the high content of volatiles in RDF (more than 70%), a large quantity of volatiles will release during RDF incineration, which is likely to cause unburnout of gaseous matters and induce the emissions (e.g., CO and dioxin) to exceed the environmental standard. The emissions (e.g., CO, SO_2, and NO_x) of pollutants, PCDDs/Fs, and heavy metals have been investigated and evaluated.[4−11] Results show that, as compared to firing pure waste, cofiring may reduce the concentration of emissions.

In coal, the content of chlorine is very low, but for RDF, the content of chlorine normally is higher. The ash compositions (Table 1) of coal and RDF are very different, and the content of alkali or alkali earth metals in RDF normally is very high. During cofiring RDF and coal, the behavior of chlorine and sulfur will be determined by the formation of gaseous HCl and SO_2 and retention of chlorine and sulfur in ash. In general, HCl emitted from a combustion process is the third important contribution to the global acidification from human activities (after SO_x and NO_x). Chlorine and sulfur can also combine with alkali or alkaline-earth metals, which are likely to form aerosols

* To whom correspondence should be addressed. Telephone: +86-10-82544231. Fax: +86-10-62561284. E-mail: xlwei@imech.ac.cn.

† Institute of Mechanics.

‡ Institute of Engineering Thermophysics.

(1) Norton, G. A.; Levine, A. D. Co-combustion of refuse-derived fuel and coal. *Environ. Sci. Technol.* **1989**, *23*, 774–783.

(2) Manninen, H.; Peltola, K.; Ruuskanen, J. Co-combustion of refuse-derived and packaging-derived fuels (RDF and PDF) with conventional fuels. *Waste Manage. Res.* **1997**, *15*, 137–147.

(3) Marton, C.; Alwast, H. Report: Operational experiences and legal aspects of co-combustion in Germany. *Waste Manage. Res.* **2002**, *20*, 476–483.

(4) Frankenhaeuser, M.; Hiltunen, M.; Manninen, H.; Palonen, J.; Ruuskanen, J.; Vartiainen, T. Emissions from co-combustion of used packaging with peat and coal. *Chemosphere* **1994**, *29*, 2057–2066.

(5) Lu, R.; Purushothama, S.; Yang, X.; Hyatt, J.; Pan, W.-P.; Riley, J. T.; Lloyd, W. G. TG/FTIR/MS study of organic compounds evolved during the co-firing of coal and refuse-derived fuels. *Fuel Process. Technol.* **1999**, *59*, 35–50.

(6) Li, H.; Yang, X.; Tomes, W.; Pan, W.-P.; Riley, J. T. Chlorinated organic compounds evolved during the combustion of blends of refuse-derived fuels and coals. *J. Therm. Anal.* **1997**, *49*, 1417–1422.

(7) Huotari, J.; Vesterinen, R. PCDD/F emissions from co-combustion of RDF with peat, wood waste, and coal in FBC boilers. *Hazard. Waste Hazard. Mater.* **1996**, *13*, 1–10.

(8) Gullett, B. K.; Dunn, J. E.; Bae, S. K.; Raghunathanet, K. Effects of combustion parameters on polychlorinated dibenzodioxin and dibenzofuran homologue profiles from municipal waste and coal co-combustion. *Waste Manage.* **1998**, *18*, 473–483.

(9) Yan, J. H.; Chen, T.; Li, X. D.; Zhang, J.; Lu, S. Y.; Ni, M. J.; Cen, K. F. Evaluation of PCDD/Fs emission from fluidized bed incinerators co-firing MSW with coal in China. *J. Hazard. Mater.* **2006**, *135*, 47–51.

(10) Manninen, H.; Perkio, A.; Palonena, J.; Peltola, K.; Ruuskanenet, J. Trace metal emissions from co-combustion of refuse derived and packaging derived fuels in a circulating fluidized bed boiler. *Chemosphere* **1996**, *32*, 2457–2469.

(11) Kouvo, P.; Backman, R. Estimation of trace element release and accumulation in the sand bed during bubbling fluidised bed co-combustion of biomass, peat, and refuse-derived fuels. *Fuel* **2003**, *82*, 741–753.

10.1021/ef800469n CCC: $40.75
Published on Web 02/10/2009

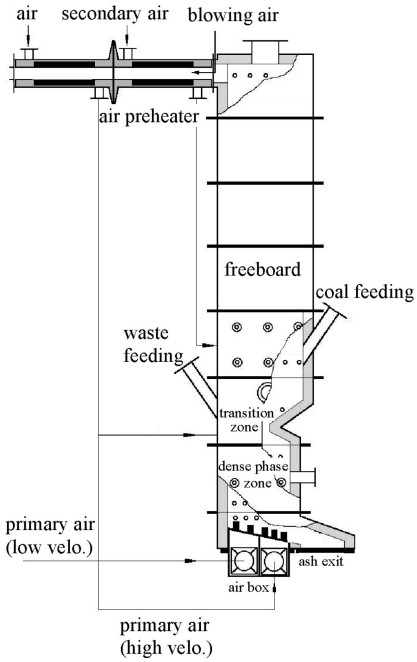

Figure 1. Schematic combustor of the internally circulating fluidized bed (ICFB).

in the flue gas.[12,13] Also, the condensed matters are very harmful in terms of causing fouling, slagging, and high temperature corrosion in the furnace.[14,15] In addition, HCl and SO_2 are known to catalyze the recombination of radicals in the flame and thus to inhibit the CO oxidation and affect the NO_x formation.[16−19] Cl_2 or Cl emitted from chlorine-containing fuel is also an important factor to form the dioxins.[20,21] Up to now, the study is still limited on the release of chlorine and sulfur for cofiring RDF and coal. Therefore, in the present article, the internally circulating fluidized bed (ICFB) was applied to investigate the behavior of chlorine and sulfur during cofiring RDF and coal.

Experimental Section

Figure 1 illustrates the schematic of the internally circulating fluidized bed incinerator. The fluidized air enters the bed via bubbling caps (0.6% orifice coefficient). Under the inclined air distributor, the plenum is separated into two equal parts. Next, the primary air separately enters the bed from air boxes with high or low air velocity. Unevenly distributed fluidized air induces a large-size internally circulating flow of solid particle in the dense bed, which may improve the properties of lateral diffusion.[22,23] Particles under the high air velocity move upward sharply and form the fluidization zone, whereas particles under the low air velocity move downward slowly and form the moving bed. The cross section of the dense phase zone is 500 × 240 mm, and the height is 1000 mm. In the furnace, the dense phase zone changes gradually into the freeboard with the cross section of 800 × 280 mm and the height of 3500 mm. Sand is used as bed materials, and the particle diameter is 0.5−1.0 mm. The air velocity is 6.0 u_{mf} in the fluidized zone with high air velocity (u_{mf} is minimum fluidized velocity) and 2.5 u_{mf} in the moving zone with low air velocity. The feeding rate of fuel was about 5−15 kg/h. During cofiring RDF and coal, the oxygen content in flue gas is 6−8%. During cofiring RDF and char, the oxygen content in flue gas is 10−16%.

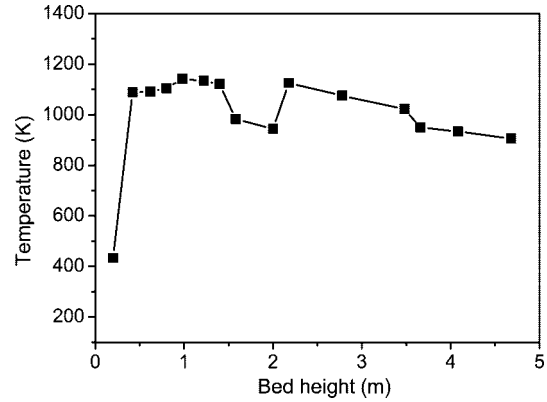

Figure 2. Gas temperature profile along the bed height during pure RDF combustion.

Figure 2 indicates the gas temperature profile along the bed height during pure RDF combustion. In the tests, the temperature is 1123−1173 K in the dense phase zone and decreases in the freeboard. The temperature is 923−1073 K at the exit. When cofiring coal or char with RDF, the bed temperature increases (sometimes to 1250 K), but the temperature in the freeboard decreases because of the less volatile content in blending fuel. Normally, char combustion mostly occurs in the bed, and volatile combustion occurs in the freeboard. When firing pure char, the temperature was 1123−1223 K in the dense phase zone and decreases in the freeboard. The temperature was 523−573 K at the exit.

When the fluidized bed is started up, first the bed is heated to about 673 K by the ignition of wood with oil. Next, the fine coal (<1 mm) is added to heat the bed to 873−973 K. Finally, coal particle is added until the bed temperature rises to about 1173 K. After the combustion is stabilized for 20−30 min, the test will begin, which will last for 30−60 min. Although two small heat transfer tubes are immersed into the sand bed, the bed temperature is mainly controlled by the balance between the heat release from burning fuel and the heat loss from gas and wall. Therefore, sometimes, a higher excess air has to be used to ensure that enough heat can be carried out by the flue gas.

A sampling probe is installed at the flue gas exit near the top of the furnace. The temperature of the sampling tube lines is heated

(12) Fernandez, A.; Wendt, J. O. L.; Wolski, N.; Hein, K. R. G.; Wang, S.; Wittenet, M. L. Inhalation health effects of fine particles from the co-combustion of coal and refuse derived fuel. *Chemosphere* **2003**, *51*, 1129–1137.

(13) Lind, T.; Kauppinen, E. I.; Hokkinen, J.; Jokiniemi, J. K.; Orjala, M.; Aurela, M.; Hillamo, R. Effect of chlorine and sulfur on fine particle formation in pilot-scale CFBC of biomass. *Energy Fuels* **2006**, *20*, 61–68.

(14) Liu, K.; Xie, W.; Li, D.; Pan, W.-P.; Riley, J. T.; Riga, A. The effect of chlorine and sulfur on the composition of ash deposits in a fluidized bed combustion system. *Energy Fuels* **2000**, *14*, 963–972.

(15) Hansen, L. A.; Frandsen, F. J.; Dam-Johansen, K.; Sørensen, H. S.; Skrifvars, B.-J. Characterization of ashes and deposits from high-temperature coal-straw co-firing. *Energy Fuels* **1999**, *13*, 803–816.

(16) Westbrook, C. K. Inhibition of hydrocarbon oxidation in laminar flames and detonations by halogenated compounds. *Nineteenth Symposium (Int.) on Combustion*; The Combustion Institute, Pittsburgh, PA, 1982; pp 127−141.

(17) Tseregounis, S.; Smith, O. I. An experimental investigation of fuel sulfur−fuel nitrogen interactions in low-pressure premixed flames. *Twentieth Symposium (Int.) Combustion*; The Combustion Institute, Pittsburgh, PA, 1985; pp 761−768.

(18) Wei, X.; Han, X.; Schnell, U.; Maier, J.; Wörner, H.; Hein, K. R. G. The effect of HCl and SO_2 on NO_x formation in coal flames. *Energy Fuels* **2003**, *17*, 1392–1398.

(19) Wei, X.; Schnell, U.; Han, X.; Hein, K. R. G. Interactions of CO, HCl, and SO_x in pulverised coal flames. *Fuel* **2004**, *83*, 1227–1233.

(20) Gullett, B. K.; Bruce, K. R.; Beach, L. O.; Drago, A. M. Mechanistic steps in the production of PCDD and PCDF during waste combustion. *Chemosphere* **1992**, *25*, 1387–1392.

(21) Tuppurainen, K.; Halonen, I.; Ruokojärvi, P.; Tarhanen, J.; Ruuskanen, J. Formation of PCDDs and PCDFs in municipal waste incineration and its inhibition mechanisms: A review. *Chemosphere* **1998**, *36*, 1493–1511.

(22) Saito, H.; Kosugi, S.; Sato, K. The revolving-type fluidized-bed incinerator-its basic performance in MSW combustion. *Waste Manage. Res.* **1988**, *6*, 261–270.

(23) Sheng, H.-Z.; Wei, X.-L.; Li, J.; Tian, W.-D.; Jin, J.; Jiang, H.-A.; Cao, J.-B.; Gao, J. The heat transfer study of external super-heater of CFB incinerator. *Environ. Eng. Sci.* **2004**, *21*, 39–44.

Table 1. Ash Composition

	ash basis (wt %)								
fuel	SiO_2	P_2O_5	CaO	K_2O	Na_2O	MgO	Al_2O_3	Fe_2O_3	TiO_2
RDF	43.6	5.0	13.11	6.1	9.11	7.74	8.76	7.29	
coal	58.72	0.22	2.7	2.05	0.12	0.54	21.26	11.22	0.84

Table 2. Fuel Properties

	chemical analysis (wt %, dry basis)					ultimate analysis (wt %, dry basis)					
fuel	moisture[a]	volatile	carbon	ash	Q_{net}[b]	C	H	O	N	S	Cl
RDF	0	73.48	9.35	17.17	24.10	57.24	9.09	14.39	0.21	0.26	1.64
coal	7.82	29.23	58.58	12.19	28.20	71.41	4.03	11.20	0.90	0.27	0.007
char	11.0	1.94	84.19	13.87	25.03	83.63	0.36	0.80	0.74	0.61	0.07

[a] As arrived. [b] Lower heating value, unit: MJ/kg.

to 453 K. Concentrations of pollutants in the flue gas were measured by Fourier transform infrared (FTIR) spectrometry (Gasmet DX-3000). In the tests, the concentrations of species H_2O, CO, CO_2, NO, N_2O, HCl, and SO_2 may be measured online with 2% error. The concentration of oxygen was measured by oxygen analyzer (TEMET 19) with 0.2% error.

Table 2 shows the fuel properties, including RDF, bituminous coal, and char. Because waste is fully dried in the process of RDF, almost no water is contained in RDF. The lower heating value of RDF is similar to that of the char. In Table 2, the content of hydrogen, oxygen, and chlorine in RDF is extremely higher than that in coal or char. The higher hydrogen and oxygen content occurs because of the organic matters in waste. Also, the higher chlorine content arises from chlorine in PVC (polyvinyl chloride) plastic and waste paper as well as from salt in food. The shape of RDF is a small rod with a diameter of 15 mm and length of 30−45 mm. The diameter of coal or char is in the range of 0.5−15 mm.

Results

Figures 3, 4, and 5 show the concentration of HCl, SO_2, or CO with varied time during pure RDF combustion (feeding 15 kg/h RDF). Because of the higher chlorine content in RDF, HCl concentration increases gradually with RDF addition. The range of HCl concentration is from 600 to 800 mg/m^3, and the variation ratio is less than 28% of the average value. However, the concentration of SO_2 or CO significantly varies, and the biggest variation ratio is 63% for SO_2 and 97% for CO emission. The average concentrations of SO_2 and CO are 152 mg/m^3 and 0.24%, respectively. Because of the very high volatile content (73%) in RDF, most gas combustion occurs in the freeboard.

In ICFB, air with high or low velocity enters the different bed zone. Gas velocity above the high velocity zone is also very high and the oxygen is insufficient in the low velocity zone, and this will affect the gas mixing in the freeboard. The poor gas mixing will inhibit the CO oxidation.

The results also indicate the pollutant emissions are significantly influenced by the various bed temperatures, the residence time, and fuel property. During data processing, we use the average value of data with varied time in the relatively stable condition.

Figures 6−9 indicate concentrations of SO_2, HCl, CO, and NO during cofiring RDF and char or coal. In Figure 6, SO_2 emission decreases with increasing RDF fraction because of lower sulfur content in RDF than in char. During cofiring RDF and coal, although the sulfur content in RDF is similar to that in coal, the curve of SO_2 in Figure 6 rises slightly with increasing RDF fraction. During cofiring RDF and char, due to higher chlorine content in RDF, the concentration of HCl approximately linearly varies with increasing RDF fraction in Figure 7. Because the volatile content in RDF is much bigger than that in char and coal, the CO concentration in Figure 8 gradually increases with increasing RDF fraction. Generally, the carbon in char or coal is mainly burned in the bed, but the volatile in RDF is combusted in the freeboard. During cofiring RDF and coal, the bed is fed more amount of fuel (15 kg/h) than that during cofiring RDF and char (<7.5 kg/h), and a lot of volatile is released into the freeboard and cannot be oxidized completely in time. Thus, CO emission is higher in cofiring RDF and coal. Figure 9 indicates the release of NO during cofiring RDF and char. NO emission increases with increasing RDF fraction. Obviously, the nitrogen in RDF may be transformed preferably as NO despite the higher nitrogen content in char.

Figures 10 and 11 indicate gaseous SO_2 and HCl conversion ratio during co-combustion with various RDF fractions. With increasing RDF ratio, the gaseous SO_2 conversion ratio slightly increases, and the HCl conversion ratio obviously decreases.

In the tests, pulverized CaO is added to absorb sulfur and chlorine during pure RDF combustion. Figures 12 and 13 give the desulfuration and dechlorination ratio with CaO addition. With increasing Ca/(S + 0.5Cl) ratio, the sulfur absorption by calcium may quickly increase. When the Ca/(S + 0.5Cl) ratio attains 2.5, the desulfuration ratio will keep stable at about 82%. As compared to the desulfuration ratio, the chlorine absorption by calcium steadily increases with increasing Ca/(S + 0.5Cl) ratio. The dechlorination ratio is less than the desulfuration ratio. It is even less than 80% when the Ca/(S + 0.5Cl) ratio attains 4.5.

Figures 14 and 15 indicate CO and NO concentration with increasing Ca/(S +0.5Cl) ratio. Calcium addition significantly depresses CO emission, while it only slightly reduces NO emission. With increasing Ca/(S + 0.5Cl) ratio, CO emission quickly decreases. When the Ca/(S + 0.5Cl) ratio attains 2.5, CO emission attains at the minimum and then almost stays stable. As compared to CO emission, NO emission decreases slightly and steadily with increasing Ca/(S + 0.5Cl) ratio.

Discussion

Effect of Chlorine Origin and Temperature on Gaseous Chlorine Species. Normally, the origin of chlorine in RDF or coal might be separated as organic and inorganic chlorine. In coal, the chlorine exists mainly as the "semi-organic" Cl: anion Cl^-, which is sorbed on the coal organic surface in pores and being surrounding by pore moisture.[24] In RDF, inorganic chlorine (NaCl, etc.) and organic chlorine (PVC, etc.) exist

(24) Yudovich, Y. E.; Ketris, M. P. Chlorine in coal: a review. *Int. J. Coal Geol.* **2006**, *67*, 127–144.

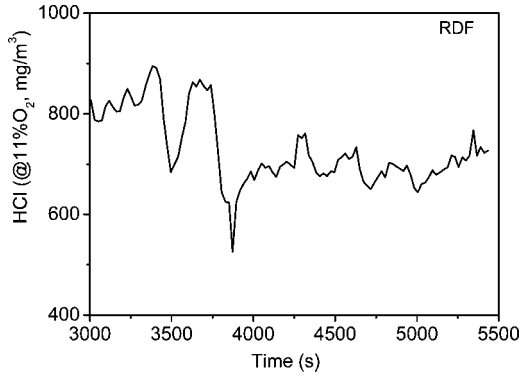

Figure 3. HCl emission with varied time during pure RDF combustion.

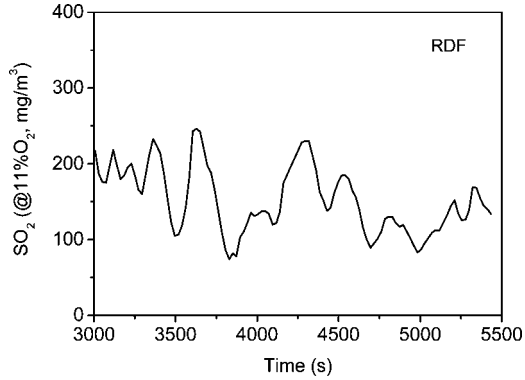

Figure 4. SO_2 emission with varied time during pure RDF combustion.

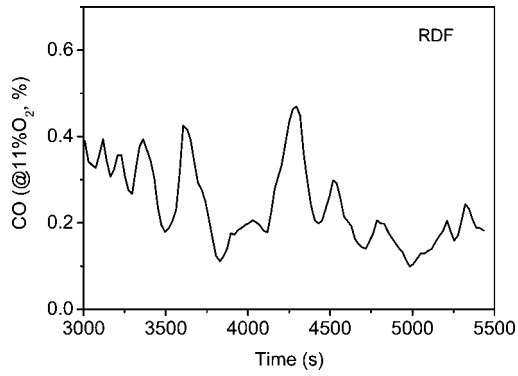

Figure 5. CO emission with varied time during pure RDF combustion.

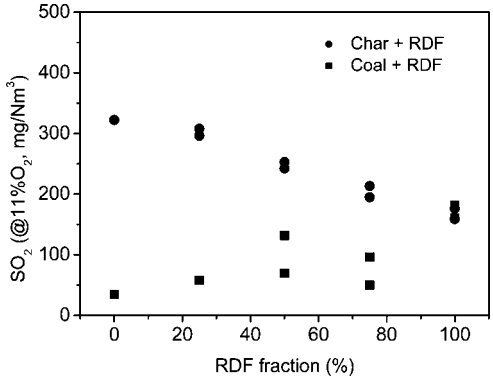

Figure 6. Release of SO_2 during cocombustion with various RDF fractions.

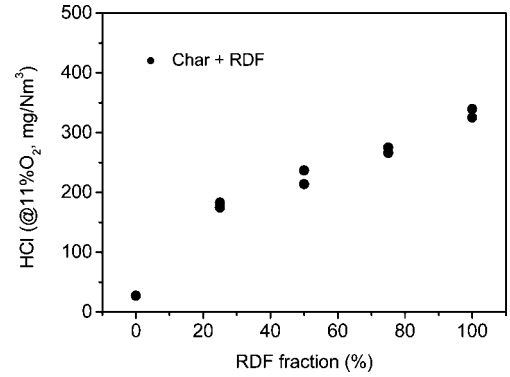

Figure 7. Release of HCl during cocombustion with various RDF fractions.

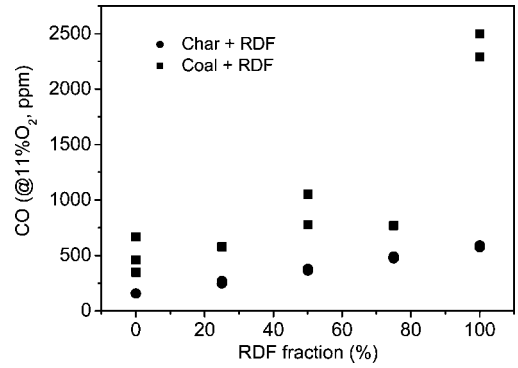

Figure 8. Release of CO during cocombustion with various RDF fractions.

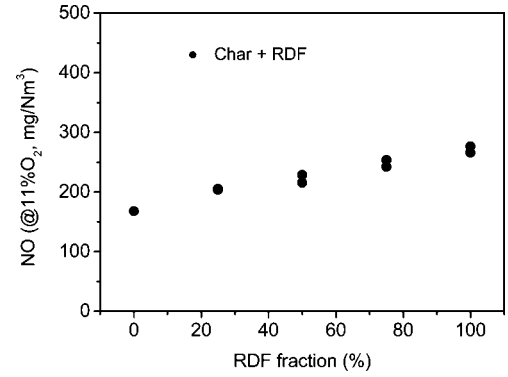

Figure 9. Release of NO during cocombustion with various RDF fractions.

together. The origin of chlorine in fuel may play a role in the release of chlorine during combustion.

The release of chlorine is also dependent on the bed temperature. At high temperature, besides HCl(g), KCl(g) and NaCl(g) might be released. Also, in the cooling process gaseous NaCl and KCl will condense on the furnace wall as solid salts, which can cause fouling, slagging, and corrosion in the furnace.[14,15] However, during the experiments, only HCl(g) might be measured by the FTIR. To analyze the release of gaseous HCl, KCl, and NaCl, the chemical equilibrium calculation is used to predict the effect of different origins on released species of chlorine and the species distribution under various temperatures.

(25) Xie, W.; Liu, K.; Pan, W.-P.; Riley, J. T. Interaction between emissions of SO_2 and HCl in fluidized bed combustors. *Fuel* **1999**, *78*, 1425–1436.

(26) Halstead, W. D.; Raask, E. The behavior of sulfur and chlorine compounds in pulverized-coal-fired boilers. *J. Inst. Fuel* **1969**, *42*, 344–349.

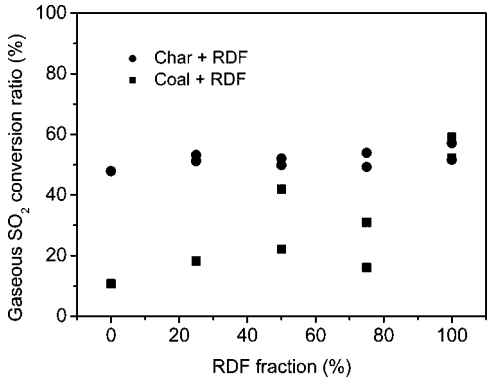

Figure 10. Gaseous SO_2 conversion ratio during cocombustion with various RDF fractions.

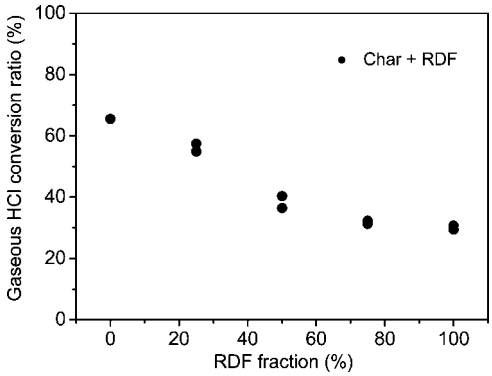

Figure 11. Gaseous HCl conversion ratio during cocombustion with various RDF fractions.

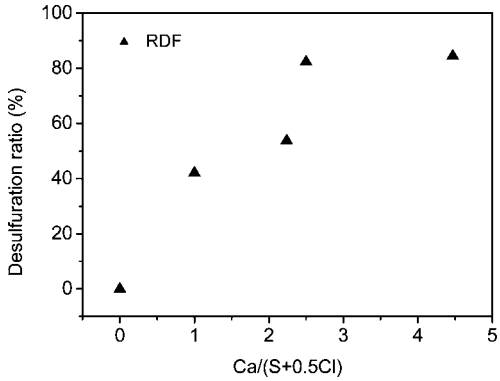

Figure 12. Desulfuration ratio with CaO addition during pure RDF combustion.

The chemical equilibrium calculation software FactSage 5.2 is used to predict the gaseous formation, which is based on the Gibbs free energy minimization approach. There are mainly two databases included in the software: FACT (compound database, over 4400 compounds) and ELEM (elements database, 90 elements). In the paper, for the system including elements C, H, O, N, S, Cl, Si, P, Ca, K, Na, Mg, Al, Fe, Ti, and Mn between 400 and 1800 K, there are 611 compounds (143 gas, 94 liquid, and 374 solid compounds) selected. The 99 main compounds (44 gaseous and 55 condensed compounds) from the calculating results are shown in Table 3. During the calculation, the excess air ratio remains at 1.6, and the coal/RDF ratio means the mass ratio. The effects of chlorine origin, temperature, and varied coal/RDF ratio are studied.

Polyvinyl chloride (PVC) and salt (NaCl) are assumed as the organic and inorganic origins of chlorine in RDF, respectively. Figure 16 gives the release ratio of chlorine in PVC and NaCl

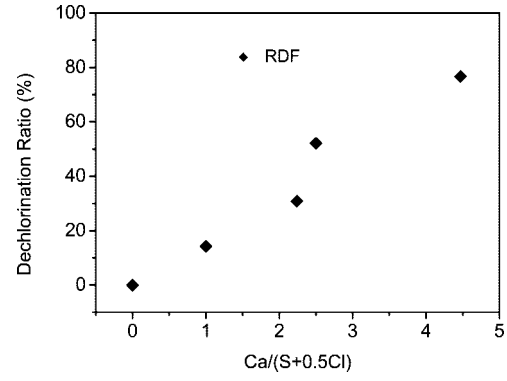

Figure 13. Dechlorination ratio with CaO addition during pure RDF combustion.

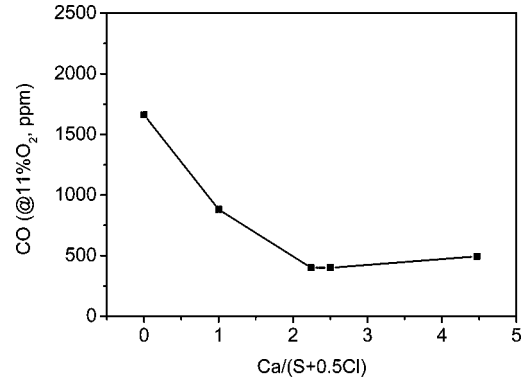

Figure 14. CO concentration with various Ca/(S + 0.5Cl) ratio.

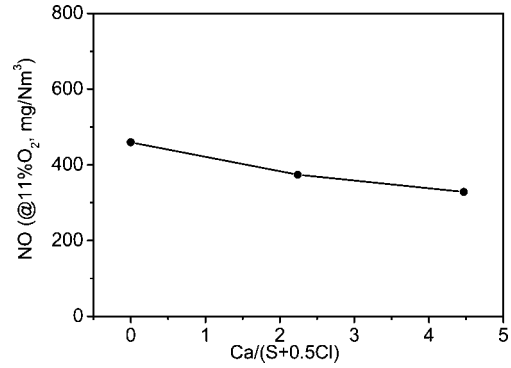

Figure 15. NO concentration with various Ca/(S + 0.5Cl) ratio.

during combustion under various temperatures. In Figure 16a, almost all of chlorine from PVC is released as gaseous HCl at the range of bed temperatures (1073−1173 K). Some of the chlorine is released as Cl_2, especially in the lower temperature. In Figure 16b, only a very small amount of chlorine from NaCl is released. The calculating results indicate that the release of HCl from organic chlorine is more dependent on the combustion temperature than that from inorganic chlorine. At the bed temperatures, organic chlorine is released more easily.

Under lower temperature, Cl_2 may form via a reaction known as the Deacon reaction:[25]

$$2HCl + \frac{1}{2}O_2 \leftrightarrow H_2O + Cl_2 \quad (1)$$

This may occur in the gas cooling process. Molecular chlorine may play an important role in the formation of dioxin.[20] On the other hand, SO_2 may be attacked by Cl_2 to form SO_3 and HCl:[25]

$$Cl_2 + SO_2 + H_2O \leftrightarrow 2HCl + SO_3 \quad (2)$$

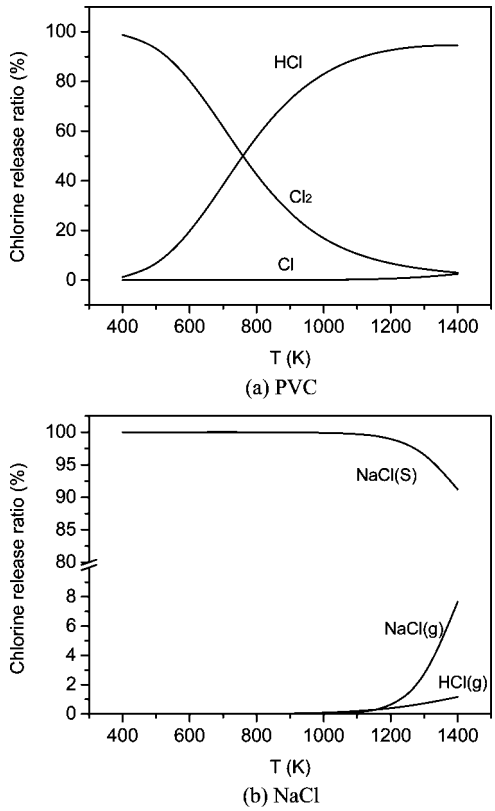

Figure 16. Distribution of the released chlorine species from PVC and NaCl during combustion.

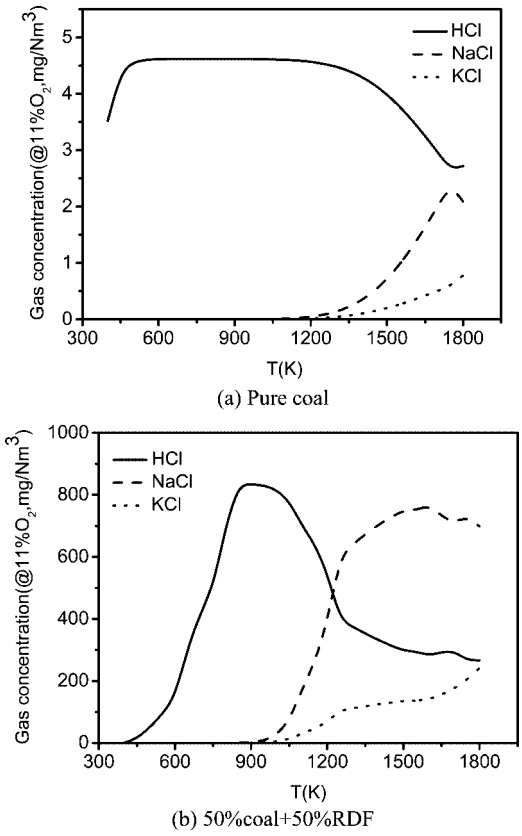

Figure 17. Distribution of the released chlorine species from cofiring coal and RDF.

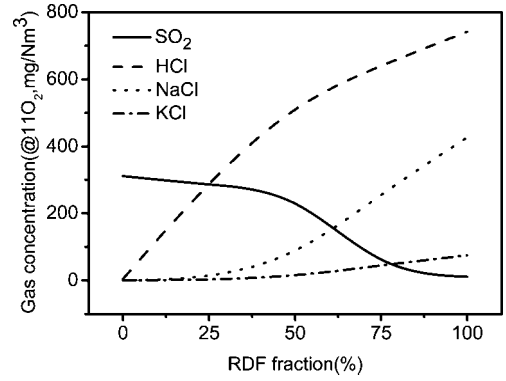

Figure 18. Distribution of the released chlorine species from cofiring coal and RDF at 1150 K.

This will decrease the formation of molecular chlorine. It indicates that the sulfur presence could suppress dioxin formation.

Figure 17a,b indicates the effect of temperature on gaseous release of HCl/NaCl/KCl with various conditions. Although Cl and Cl_2 are also two important species containing chlorine, the results show that their concentrations are over one magnitude smaller than that of HCl/NaCl/KCl, and they are not shown in the figures. It indicates that the existence of SO_2 will result in less formation of Cl and Cl_2. In Figure 17a, it can be seen that the release of HCl remains nearly stable during 500 and 1200 K when the coal is burned. In Figure 17b, when cofiring coal and RDF, the gaseous HCl concentration increases quickly and then decreases sharply, and the maximum concentration of HCl is attained at about 900 K. Gaseous NaCl and KCl begin to release from about 900 K. In the practical FBC furnace, the gaseous NaCl and KCl release from the dense phase zone. Once temperature decreases along the bed height, NaCl and KCl will adhere to the furnace wall as solid salts, which perhaps erode the metal wall. Thus, the release of gaseous alkali metal should be controlled during combustion.

Considering that the temperature in the dense phase zone is 1123−1173 K in the tests, 1150 K is chosen as the reaction temperature for calculation to study the formation of SO_2/HCl/NaCl/KCl in the furnace, and the results are shown in Figure 18. During cofiring coal and RDF, with increasing RDF content, gaseous NaCl and KCl increase steadily. In pure RDF combustion, the fraction of chlorine release as NaCl and KCl nearly approaches that of HCl.

Release of HCl and Its Retention by Additional CaO. The results of Figure 11 may be explained by the origin and content of chlorine, sulfur, and alkaline metals in coal or RDF. During RDF combustion in ICFB, the chlorine from PVC is released more easily as HCl. Also, NaCl in fuel may induce the following reaction:[26,27]

$$2NaCl(liq) + SO_2(g) + H_2O(g) + 0.5O_2(g) \leftrightarrow Na_2SO_4(g) + 2HCl(g) \quad (3)$$

For cofiring char with RDF ratio less than 25%, SO_2 emission is higher than HCl emission. The above reaction results in more HCl emission from the inorganic chlorine. With increasing RDF ratio, SO_2 emission deceases and HCl emission increases, and thus the above reaction becomes less important and the chlorine might be retained by the reaction:[28]

$$CaO(s) + 2HCl(g) \leftrightarrow CaCl_2(s,l) + H_2O(g) \quad (4)$$

Obviously, the gaseous HCl conversion ratio is determined by the chlorine content and origin as well as the competition between reactions 3 and 4. The change of gaseous SO_2 conversion ratio might be explained by these factors, but is

Table 3. Main Species Used in the Thermodynamic Equilibrium Calculation

category	species
gas species (44)	O_2, OH, H_2O, CO, CO_2, Na, NaO, NaOH, $(NaOH)_2$, SO, SO_2, SO_3, $O_2S(OH)_2$, Na_2SO_4, Cl, Cl_2, HCl, ClO, HOCl, COCl, $COCl_2$, ONCl, NaCl, $(NaCl)_2$, MgCl, $MgCl_2$, OAlCl, $SOCl_2$, K, KO, KOH, $(KOH)_2$, K_2SO_4, KCl, $(KCl)_2$, $Ca(OH)_2$, $CaCl_2$, $TiOCl_2$, $MnCl_2$, FeCl, $FeCl_2$, $FeCl_3$, $(FeCl_2)_2$, $NaFeCl_4$
condensed species (55)	Na_2SO_4(liq), $K_2Si_4O_9$(liq), $CaSiTiO_5$(liq), $Na_2Mg_2Si_6O_{15}$(s), $NaAlSiO_4$(s3), $NaAlSiO_4$(s4), $NaAlSi_3O_8$(s2), $Na_3(PO_4)$(s), Na_2SO_4(s, s2), $MgSO_4$(s), $MgSO_4(H_2O)$(s), NaCl(s), KAl_9O_{14}(s), $K_2Si_2O_5$(s), $K_2Si_2O_5$(s2), $K_2Si_4O_9$(s, s2), $KAlSi_2O_6$(s, s2), $KAlSi_3O_8$(s2), $KAl_3Si_3O_{10}(OH)_2$(s), $KMg_3AlSi_3O_{10}(OH)_2$(s), K_2SO_4(s, s2), $KAl(SO_4)_2$(s), KCl(s), CaO(s), $CaCO_3$(s2), $CaMg(CO_3)_2$(s), $CaAl_2O_4$(s), $Ca_3Al_2O_6$(s), $CaSiO_3$(s, s2), Ca_2SiO_4(s, s2), Ca_3SiO_5(s), $Na_2Ca_2Si_3O_9$(s), $Na_2Ca_3Si_6O_{16}$(s), $CaOMgOSiO_2$(s), $MgOCaOSi_2O_4$(s), $MgOCa_2O_2Si_2O_4$(s), $MgOCa_3O_3Si_2O_4$(s), $CaAl_2Si_2O_8$(s2), $Ca_3Al_2Si_3O_{12}$(s), $Ca_3(PO_4)_2$(s, s2), $Ca_5HO_{13}P_3$(s), $CaSO_4$(s), $CaCl_2$(s), $CaTiO_3$(s, s2), $CaSiTiO_5$(s), $Ca_2Fe_2O_5$(s), $Ca_3Fe_2Si_3O_{12}$(s)

more complicated. In addition, sulfur is likely to be absorbed by calcium and magnesium in ash under fluidized bed temperature.

On the other hand, HCl capture in bed depends very strongly on bed temperature. Reaction 4 is strongly reversible at typical FBC conditions.[29] Actually, HCl capture will be very limited at normal bed temperatures. In addition, $CaCl_2$ may also react with SO_2 via the reactions:

$$CaCl_2 + SO_2 + O_2 \leftrightarrow CaSO_4 + Cl_2 \quad (5)$$

$$CaCl_2 + SO_2 + H_2O \leftrightarrow CaSO_4 + 2HCl \quad (6)$$

It will induce HCl and Cl_2 to be released again from the bed.

The adsorption of HCl by additional CaO can be described by reaction 4, which is significantly dependent on the temperature. As temperature increases, the chlorination of CaO goes through a maximum at around 873 K.[30] With increasing the temperature to 1073−1173 K (at FBC state), relatively little adsorption may be possible. For example, at 1073 K only 30% conversion of the limestone was reported.[31] Obviously, the adsorption is limited by chemical equilibrium between gas and solid. In the results of Figures 12 and 13, the dechlorination ratio is less than the desulfuration ratio, especially for the lower Ca/(S + 0.5Cl). When Ca/(S + 0.5Cl) is higher than 4, the dechlorination ratio rises to about 80%. This may be explained by the adsorption in freeboard. When more CaO is added, some of pulverized CaO may flow into the freeboard, where the adsorption may occur preferably because of relatively low temperature.

Effect of Additional CaO and HCl on CO and NO Emission. There are two factors that might have influences on NO and CO emission when adding CaO. One is the catalysis of CaO and char on the reaction of NO and CO as follows:[32]

$$NO + CO \xrightarrow{CaO} \frac{1}{2}N_2 + CO_2 \quad (7)$$

$$NO + CO \xrightarrow{char} \frac{1}{2}N_2 + CO_2 \quad (8)$$

Under the conditions with high CO concentration (>1000 ppm), CaO and char will catalyze the reaction of NO and CO. Therefore, CaO addition will reduce NO and CO emission. Another factor is the influence of HCl on the NO and CO emission.[33−35] HCl may significantly inhibit CO oxidation to increase CO emission. Therefore, increasing the Ca/(S + 0.5Cl) ratio will reduce HCl emission and decrease CO emission (see Figure 14). The influence of HCl on NO emission is still not clear.[34,35] The results of Lu et al. indicate that chlorine increases NO emission in FBC.[34] Yet Gokulakrishnan and Lawrence found that HCl addition may reduce NO formation.[35] In Figure 15, it can be seen that the influence of HCl on NO emission is not significant and an increasing Ca/(S + 0.5Cl) ratio slightly decreases NO emission.

Conclusions

The release of chlorine and sulfur during the cofiring of RDF and coal is investigated in ICFB. The concentration of SO_2, HCl, or CO significantly varies in pure RDF combustion. Although the sulfur content in RDF is similar to that in coal, the concentration of SO_2 is a little less than that in pure RDF combustion. During cofiring RDF and char, the concentration of HCl approximately linearly varies with increasing RDF fraction. Because the volatile content in RDF is much higher than that in coal, the CO concentration gradually increases with increasing RDF fraction.

(27) Wei, X. L.; Lopez, C.; von Puttkamer, T.; Schnell, U.; Unterberger, S.; Hein, K. R. G. Assessment of chlorine−alkali−mineral interactions during co-combustion of coal and straw. *Energy Fuels* **2002**, *16*, 1095–1108.

(28) Partanen, J.; Peter Backman, P.; Backman, R.; Hupa, M. Absorption of HCl by limestone in hot flue gases. Part I: the effects of temperature, gas atmosphere and absorbent quality. *Fuel* **2005**, *84*, 1664–1673.

(29) Zhang, C. X.; Wang, Y. X.; Yang, Z. H.; Xu, M. H. Chlorine emission and dechlorination in co-firing coal and the residue from hydrochloric acid hydrolysis of *discorea zingiberensis. Fuel* **2006**, *85*, 2034–2040.

(30) Lawrence, A. D.; Bu, J. The reactions between Ca-based solids and gases representative of those found in a fluidized-bed incinerator. *Chem. Eng. Sci.* **2000**, *55*, 6129–6137.

(31) Weinell, C. E.; Jensen, P. I.; Dam-Johansen, K.; Livbjerg, H. Hydrogen chloride reaction with lime and limestone: Kinetics and sorption capacity. *Ind. Eng. Chem. Res.* **1992**, *31*, 164–171.

(32) Johnsson, J. E. A kinetic model for NO_x formation in fluidized bed combustion. *Proceedings of the 11th International Conference on Fluidized Bed Combustion*; ASME, New York, 1989; pp 1111−1118.

(33) Anthony, E. J.; Bulewicz, E. M.; Janicka, E.; Kandefer, S. Chemical links between different pollutant emissions from a small bubbling FBC. *Fuel* **1998**, *77*, 713–728.

(34) Lu, D. Y.; Anthony, E. J.; Talbot, R.; Winter, F.; Löffler, G.; Wartha, C. Understanding of halogen impacts in fluidized bed combustion. *Energy Fuels* **2001**, *15*, 533–540.

(35) Gokulakrishnan, P.; Lawrence, A. D. An experimental study of the inhibiting effect of chlorine in a fluidized bed combustor. *Combust. Flame* **1999**, *116*, 640–652.

The release ratio of chlorine and sulfur is mainly dependent on the temperature and alkaline metal in fuel ash. HCl capture will be very limited at normal bed temperatures and thus may require some other way to control it. With the CaO addition, the sulfur absorption by calcium quickly increases, and the desulfuration ratio is bigger than the dechlorination ratio. Calcium addition significantly depresses CO emission, while it only slightly reduces NO emission.

The equilibrium calculations show that organic chlorine is released more easily than is inorganic chlorine at the bed temperatures. Gaseous HCl emission increases with increasing RDF fraction, and gaseous KCl and NaCl formation might occur from about 900 K.

Acknowledgment. Financial support by the National Natural Science Foundation of China (Project Nos. 50776099 and 50376068) is gratefully acknowledged. We also thank Prof. Qinggang Lu and Yongjie Na as well as Dr. Cheng Qin for their help on this work.

EF800469N